(19) Europäisches Patentamt
European Patent Office
Office européen des brevets

(11) EP 1 305 601 B1

(12) **EUROPEAN PATENT SPECIFICATION**

(45) Date of publication and mention of the grant of the patent:
21.12.2005 Bulletin 2005/51

(21) Application number: **01942160.1**

(22) Date of filing: **08.06.2001**

(51) Int Cl.[7]: **G01N 21/47**, G02B 21/14, A61B 5/00

(86) International application number:
PCT/US2001/018721

(87) International publication number:
WO 2001/094913 (13.12.2001 Gazette 2001/50)

(54) **PHASE DISPERSIVE TOMOGRAPHY**

PHASENDISPERSIVE TOMOGRAPHIE

TOMOGRAPHIE A DISPERSION DE PHASE

(84) Designated Contracting States:
AT BE CH CY DE DK ES FI FR GB GR IE IT LI LU MC NL PT SE TR

(30) Priority: **09.06.2000 US 591297**

(43) Date of publication of application:
02.05.2003 Bulletin 2003/18

(73) Proprietor: **MASSACHUSETTS INSTITUTE OF TECHNOLOGY**
Cambridge, MA 02139 (US)

(72) Inventors:
- **YANG, Changhuei**
  Durham, North Carolina 27708 (US)
- **WAX, Adam**
  Boston, MA 02139 (US)
- **FELD, Michael, S.**
  Newton, MA 02468 (US)

(74) Representative: **Greenwood, John David et al**
Graham Watt & Co LLP
St Botolph's House
7-9 St Botolph's Road
Sevenoaks Kent TN13 3AJ (GB)

(56) References cited:
WO-A-01/84124

- **YANG C ET AL: "FEASIBILITY OF FIELD-BASED LIGHT SCATTERING SPECTROSCOPY" OFFSHORE, INDUSTRIAL PUBLICATIONS, CONROE, TX,, US, vol. 5, no. 2, April 2000 (2000-04), pages 138-143, XP001051328 ISSN: 0030-0608**
- **CHANGHUEI YANG ET AL: "Phase-dispersion optical tomography" OPTICS LETTERS, 15 MAY 2001, OPT. SOC. AMERICA, USA, vol. 26, no. 10, pages 686-688, XP002186713 ISSN: 0146-9592**
- **YANG C ET AL: "Measurement of the anomalous phase velocity of ballistic light in a random medium by use of a novel interferometer" OPTICS LETTERS, 15 FEB. 2001, OPT. SOC. AMERICA, USA, vol. 26, no. 4, pages 235-237, XP002186714 ISSN: 0146-9592**
- **CHANGHUEI YANG ET AL: "Interferometric phase-dispersion microscopy" OPTICS LETTERS, 15 OCT. 2000, OPT. SOC. AMERICA, USA, vol. 25, no. 20, pages 1526-1528, XP002186715 ISSN: 0146-9592**

EP 1 305 601 B1

Description

BACKGROUND OF THE INVENTION

[0001] Ballistic light is defined as the light which traverses a scattering medium in the same direction as the incident light. Conventionally, ballistic propagation is pictured as photons which are undeflected in transmission. Such a picture, henceforth called the photonic model, is extensively used in optical tomography, and it explains many properties of ballistic propagation. For example, the photonic model explains the emergence of ballistic light from a thick turbid medium at an earlier time than the scattered light. However, this model is incomplete, as the wave nature of the light is not considered.

[0002] Interferometers have been used to measure phase changes based on fluctuations in path length. Phase measurements using interference microscopes, for example, have been used previously to provide two dimensional images of thin tissue samples.

[0003] However, there is a continuing need for improvements in systems and methods for measuring turbid media such as tissue.

SUMMARY OF THE INVENTION

[0004] The phase velocity of light traversing a diffuse scattering medium is a function of scatterer size. To measure this effect optically, an interferometer that measures very small differences in phase velocity between at least two harmonically related wavelengths is used, such as 800 and 400 nm, for example. One wavelength that is an integer multiple of the other wavelength can thus be used to provide quantitative phase information regarding a scanned region of interest. A pair of such wavelengths can be generated harmonically or by using two separate light sources which satisfy the integer multiple requirement to within 5% of the lowest wavelength, i.e. one wavelength is about an integer multiple of the other wavelength. In a preferred embodiment, the interferometer system of the present invention is sensitive to phase velocity differences at least of 40 m/s in a 2 cm thick turbid sample, for example, or equivalently an optical path length difference of about 5nm. This sensitivity provides for the measurement of very dilute turbid media, a more relevant model for optical applications such as biomedical imaging and remote sensing through atmospheric conditions such as smoke or fog.

[0005] The variations in phase velocity result from the wave nature of ballistic propagation and can be measured by treating the ballistic electromagnetic field as the interference of the input light field with the scattered field. Using van de Hulst and Mie scattering theories, ballistic propagation separates into three regimes: (1) When the scatterer size (a) is much smaller than the optical wavelength (λ), the turbid medium may be approximated as a bulk medium for phase velocity considerations; (2) when a is comparable to λ, the phase velocity is strongly dependent on scatterer size; (3) when a is much larger than λ, turbidity can be ignored for phase velocity considerations. Consequently, by measuring tissue with appropriate harmonically related wavelengths of light, the size and distribution of cellular structures within the tissue can be measured.

[0006] Ballistic light can propagate with a phase velocity that is uncharacteristic of the constituent materials of the turbid medium. Hence, the ballistic light itself must carry phase information about the structure and composition of the turbid medium. The photonic model simply cannot explain this variation in phase velocity.

[0007] A preferred embodiment of the invention relates to a microscopy imaging system referred to herein as phase dispersion microscopy (PDM). This system is based on measuring the phase difference between a fundamental wavelength of light and a harmonic of unscattered light that are transmitted through a medium. PDM employs an interferometer that substantially reduces or eliminates noise due to optical path length fluctuations. In other phase measurement techniques, it is difficult to account for minute interferometer path length differences in the measured phase. Thus, without an independent way of eliminating such jitter, phase measurements cannot directly yield physically relevant information. In contrast, the phase measured in the present system is independent of path length errors. As an example, the system is used to measure very small anomalous phase velocity differences experienced by ballistic light during propagation through turbid media. The present system and method can provide quantitative information by measuring the refractive index dispersion of very dilute material such as DNA-water solutions. The sensitivity of the technique and its image formation capabilities can be applied of the imaging of an unsustained tissue section.

[0008] This technique can be used to provide two dimensional (2D) or three dimensional (3D) imaging of tissue both *in vitro* and *in vivo.* Additional details regarding the systems and methods of the invention can be found in WO 01/84124 A2.

YANG C ET AL: 'FEASIBILITY OF FIELD-BASED LIGHT SCATTERING SPECTROSCOPY' OFFSHORE, INDUSTRIAL PUBLICATIONS, CONROE, TX,, US, vol. 5, no. 2, April 2000 (2000-04), pages 138-143, ISSN: 0030-0608 discloses the closest prior art.

BRIEF DESCRIPTION OF THE DRAWINGS

[0009] The file of this patent contains at least one drawing executed in color. Copies of this patent with color drawings will be provided by the Patent and Trademark Office upon request and payment of the necessary fee.

Figure 1 illustrates a phase measurement system in accordance with the invention including mirrors, M1 and M2, and a beamsplitter BS. D1 and D2 are photodetectors, and DM is a 400 nm/800 nm dichroic mirror.
Figure 2 illustrates phase velocity difference versus scatterer radius.
Figure 3 graphically illustrates a representation of modeled normalized phase velocity, $\frac{\Delta v}{\eta v_0}$ versus normalized scatter size, ρ where the normalized refractive index difference, (*m-1*), equals 0.2 for this particular example.
Figure 4 is another preferred embodiment of the invention using mirrors, M1 and M2, a beamsplitter BS, microscopic objective lens 01, 02, 03 and 04, photodetectors D1 and D2, and a 400 nm/ 800 nm dichroic mirror DM.
Figure 5 compares images from a phasecontrast system (top) and PDM (bottom) of a drop of water and a drop of 1.0% DNA solution sandwiched between 2 covers slips in which the measured refractive index dispersion, (Δn_{400nm} - Δn_{800nm}), of the DNA solution was $(1.3\pm0.2)x10^{-4}$.
Figure 6A includes images of a white matter - gray matter interface in a 16 μm thick brain sample with the top being a phase contrast image, the middle being a phase dispersion image in accordance with the present invention and the bottom image being an adj acent frozen section stained with hemotoxylin and eosin.
Figure 6B compares the 3D imaging of the present invention with standard OCT images.
Figure 7 illustrates systems used for imaging of tissue in accordance with the invention.
Figure 8 illustrates the use of a fiber optic system in accordance with the invention.

[0010] The foregoing and other objects, features and advantages of the invention will be apparent from the following more particular description of preferred embodiments of the invention, as illustrated in the accompanying drawings in which like reference characters refer to the same parts throughout the different views. The drawings are not necessarily to scale, emphasis instead being placed upon illustrating the principles of the invention.

DETAILED DESCRIPTION OF THE INVENTION

[0011] The measurements are made using a low-coherence phase dispersion interferometer 10 shown in Figure 1. The input light 12 is created by superposing beams of laser light at the fundamental and preferably the second harmonic frequencies. The source 14 can be a low coherence Ti:sapphire laser producing 150 fs pulses at 800 nm, and the second harmonic is generated by a standard frequency doubler. The superposed beam is split into two components at the beamsplitter 16. One component makes two passes through the turbid medium 18 in the signal arm of the interferometer with mirror M2. The other component passes through a compensator cuvette of water 15 and reflects from a reference mirror M1 in the reference arm. The reference mirror M1 moves at a constant velocity 20 and induces a Doppler shift on the return beam. The recombined beams are then separated by wavelength using a dichroic mirror DM and measured separately by photodetectors D1 and D2. The resulting heterodyne signals at both wavelengths are measured and digitized by a 16-bit 100 kHz A/D converter 24 and further processed and stored in memory with data processor 26. Each digitized signal is bandpassed around its center heterodyne frequency, given by the Doppler shift. The filtered signals are then Hilbert transformed, and the respective phases Ψ_1 (fundamental) and Ψ_2 (second harmonic) are extracted. Related phase techniques have been used to measure the dispersion of metals and the refractive index of air.

[0012] In a conventional interferometer, path length fluctuations as small as a tiny fraction of a wavelength will vary the measured phase significantly; therefore, without an independent way of eliminating such jitter, phase measurements cannot directly yield physically relevant information. However, it can be seen that jitter of magnitude Dx in either the signal or reference arm of our interferometer will vary the phases, Ψ_1 and Ψ_2, by $k_1\Delta x$ and $k_2\Delta x$, respectively, with k_1 and k_2 the free space wavenumbers of the fundamental and second harmonic light beams. Since k_2 is exactly double k_1, the effect of jitter can be totally eliminated by subtracting twice Ψ_1 from Ψ_2. Note that such elimination is only possible when one wavelength is an integer multiple of the other. This operation yields, $\Delta L_{k2,k1}$, the difference in optical path lengths of the two wavelengths in the interferometer, with great sensitivity:

$$\Delta L_{k2,k1} = \frac{\Psi_2 - 2\Psi}{k_2}. \quad (1)$$

In the experiments presented below, the sensitivity achieved is about 5 nm in optical path length difference or, equivalently, about $9x10^{-2}$ rad in phase difference with respect to the second harmonic light.

[0013] In a preferred embodiment, the phase of light traversing a 10 mm thick turbid medium composed of scattering polystyrene spheres in water can be measured. A water filled cuvette of the same thickness provides phase compensation. Note that because the ballistic light makes two trips through the cuvette, the effective thickness, L, is 20 mm. Polystyrene microspheres of a given size are gradually added to the signal arm cuvette, and the changes in optical path difference are measured. The fractional volume of microspheres, η, is varied from 8×10^{-6} to 3×10^{-3}. The relative refractive index of the microspheres is 1.20 at 800 nm and 1.23 at 400 nm, with respect to that of water. Each measurement of optical path difference is then used to find the fractional phase velocity difference, $\frac{\Delta v_2}{v_2} - \frac{\Delta v_1}{v_0}$, between the two wavelengths in the cuvette:

$$\frac{\Delta v_2}{v_0} - \frac{\Delta v_1}{v_0} = -\frac{\Delta L_{k2,k1}}{n_0 L}, \tag{2}$$

with v_o the speed of light in water and n_0 the refractive index of water. Note that second order corrections due to dispersion of water and turbidity are omitted, as they have minimal impact on the calculation. Our system can measure fractional changes in phase velocity difference as small as 2 parts in 10^7. Measurements are made for a succession of microspheres varying in radius from 10 nm to 10 mm. The data points of Figure 2 show the measured fractional difference in phase velocities as a function of scatterer size.

[0014] The transmission of the ballistic light through the turbid medium can be characterized by a complex index of refraction $n_{cx} = n - in'$. The ballistic light field, $E(L)$, which has traversed a distance L in the turbid medium, can be written as a complex exponential attenuation of the incident field, $E(0)$:

$$E(L) = E(0)e^{-ikn_{ex}L} = E(0)e^{-ikn(n-in')L}, \tag{3}$$

with k the wavenumber in the surrounding medium. The components of the refractive index can be expressed in terms of $S(0)$, the scattering function evaluated in the exact forward direction of the input light:

$$n = 1 + \frac{2\pi N}{k^3} Im(S(0)), \tag{4a}$$

$$n' = \frac{2\pi N}{k^3} Re(S(0)), \tag{4b}$$

with N the number of scatterers per unit volume.

[0015] The imaginary part of the refractive index is associated with the well-known attenuation of ballistic light due to scattering and has been extensively studied. Note that, as determined by the optical theorem, attenuation occurs in the forward direction, even for non-absorbing particles. However, the effect of scatterers on the real part of the refractive index cannot be readily measured; to induce a change in n which is measurable by conventional methods requires such a large value of N that there is too little ballistic light to detect. The present interferometer allows us to circumvent this problem by providing a much more sensitive means of measurement. Thus, we can study subtle variations of the imaginary part of the scattering function.

[0016] To elucidate the effect of spherical scatterers on the refractive index (or, equivalently, the associated phase velocity), consider the van de Hulst scattering representation for spheres of radius α and refractive index m relative to the surrounding medium. In this representation, straight rays are traced through a spherical scatterer and assumed not to deviate during entry and exit. This is strictly valid only when the scatterer size is large compared to the wavelength and the refractive index difference is small. Nevertheless, it provides important physical insights and, as shown below, describes the salient features well beyond these limits. For light at one wavelength, the van de Hulst representation gives a fractional phase velocity change of the form:

$$\frac{\Delta v}{v_0} = 1 - n = -\frac{3\eta}{2a^3k^3}(ka)^2\left(\frac{\sin\rho}{\rho^2} - \frac{\cos\rho}{\rho}\right), \quad (5)$$

with $\rho=2ka(m-1)$ the normalized scatterer size, and $(m-1)$ the relative refractive index difference between the scatterers and the surrounding medium. A plot of $\frac{\Delta v}{\eta v_0}$ using the van de Hulst representation is shown in Figure 3. For comparison, an exact computation based on Mie theory is also shown.

[0017] Figure 3 reveals three different regimes of ballistic light propagation, depending on the scatterer properties. Consider each of these analytically using the van de Hulst representation:

1. $\rho << 1$ - turbid medium as bulk medium.

[0018] In this limit, Eq. (5) reduces to:

$$\Delta v = -\eta v_0(m-1) \quad (6)$$

In this case, the change in phase velocity arises only from bulk refractive index change due to the presence of small scatterers. From another perspective, when the phase lag through each scatterer is small, the net result is simply an overall change in phase velocity, as determined by the refractive index difference.

II. $\rho \approx 1$ - no simplification.

[0019] In this regime Eq. (5) cannot be simplified. The phase velocity is seen to oscillate with changing ρ. The net change in phase velocity is strongly dependent on whether the forward scattered light is in phase or out of phase with the input light. Note the existence of an anomalous phase velocity increase for some values of ρ, despite the fact that the scatterers have *higher* refractive index than water. In this situation, the effective refractive index of the medium is *reduced* by the addition of material with higher refractive index.

III $\rho >> 1$ - phase velocity is independent of turbidity.

[0020] In this limit, Eq. (5) reduces to:

$$\Delta v\text{-}0 \quad (7)$$

The phase velocity is thus independent of the presence of turbidity. This is the only regime in which the photonic model provides a complete description. Physically, we can understand this from the fact that when ρ is large, the phase of the transmitted light varies rapidly with increasing distance from the center of the sphere. The net result is that the phase shift of the transmitted light averages to zero.

[0021] The above is based on the behavior of ballistic propagation for light of a single wavelength. Based on phase velocity differences between two wavelengths, the three regimes still can be clearly seen (Figure 2). The predicted phase velocity variation calculated from the van de Hulst representation, and the exact solution derived from Mie theory, are also shown in Figure 2. The van de Hulst representation, though approximate, gives a good fit to the measured data.

[0022] The phase velocity difference of the two wavelengths reveals an additional phenomenon that is absent in single wavelength behavior, a dramatic region of negative dispersion (relative to water). Paradoxically, the negative dispersion is caused by the addition of appropriately sized *positive* dispersion scatterers. This effect is due to the shift in the phase velocity profile arising from the scaling of p with wavelength. Note that it is not dependent on the anomalous phase velocity increase discussed above.

[0023] The distinctive features of the phase velocity difference profile makes it possible to extract precise scatterer size distributions in polydisperse media, by scanning the fundamental/second harmonic wavelengths. The high precision is afforded by the extremely high sensitivity achieved with phase-based measurements. This method complements related intensity-based techniques for measuring the size distribution of cell nuclei, an important indicator of pre-can-

cerous changes in biological tissues. The phase dispersion measurement method described here can also form the basis of an imaging technique which is complementary to conventional phase contrast microscopy (PCM). In this case, image formation is based on the phase shift of ballistic light traversing the specimen. The use of ballistic light reveals a different type of information about the tissue compared to PCM, where the measured quantity is derived from scattered light. The present invention performs better than PCM in dispersive and weakly scattering tissues.

[0024] In this embodiment an interferometer 28 seen in Figure 4, microscope objectives 03 and 04 focus the beam onto the sample such as excised tissue with a FWHM of about 7 μm at both wavelengths, however, there can be difficulty in aligning the returning path to overlap with the incoming path degrades the resolution to about 10 microns. A finer resolution can be achieved by using higher power objectives and improved alignment. The reference mirror moves at a constant velocity of 1mm/s and induces a Doppler shift on the returning beam. As before, the two composite beams then are recombined, separated by their wavelength components with dichroic mirror, and measured separately by photodetectors.

[0025] To illustrate the sensitivity of this method, the refractive index dispersion change was measured by adding a small amount of DNA to water. The measurement is performed by replacing the microscope objectives (O1 and 02), and the sample with a cuvette of very dilute herring testes DNA (0.014% vol. conc.). In this particular example, the cuvette is 10 mm thick, which makes L=20 mm due to the system's double pass configuration. The compensator 30 and its associated objectives (O3 and O4) are correspondingly replaced by a cuvette containing only water. The measured refractive index dispersion, based on 10 separate measurements, is $(2.27\pm0.04)\times10^{-6}$.

[0026] Existing techniques provided a qualitative measurement resulting in an image where it is difficult to separate the contributions from absorption and phase shift. The present invention provides a quantitative measurement of the phase shift. In addition, existing techniques relied on small phase shifts between the scattered and unscattered light from the target for contrast, whereas the present invention directly measures the small phase shifts of the unscattered light associated with the refraction of the target. This results from the fact that interference-based techniques detect unscattered light far more efficiently than scattered light. Therefore, the present method can be applied to situations for which quantitative characterizations are required and where there is little or no scattering.

[0027] As an illustration, compare the performance of the method of prior phase contrast techniques to the method of the present invention on similarly prepares samples comprising a drop of water and a drop of DNA solution (1.0% vol. conc.) sandwiched between two cover slips. The separation between the cover slips is 170 μm. As evident in the lower image generated using a prior technique of Figure 5, PDM can easily distinguish the two drops and provides a refractive index dispersion value for the DNA solution. In contrast, the upper image generated using a prior technique does not distinguish between the two. Interestingly, the refractive index dispersion measured in the experiment, $(1.3\pm0.2)\times10^{-4}$ differs from the value, 1.6×10^{-4}, extrapolated from the cuvette measurement, based only on the ratio of their concentrations. This difference can be attributed to the fact that the refractive index depends on scatterer size, as well as concentration. Thus, at higher concentration, the formation of DNA aggregater, which behave as scatterers, effectively alters the refractive index.

[0028] To further illustrate the present phase dispersion method to images of a brain tissue sample. A 16 μm thick sample was prepared from a frozen brain tissue block using a microtome. The sample was obtained from the autopsy material of an Alzheimer disease patient. A drop of glycerol was applied to keep the sample moist and to provide index matching. Figure 6A shows phase contrast (top) and phase dispersion (middle) images taken from the same sample. For comparison, a stained sample from an adjacent thin section is also shown in the lower image. As can be seen, the phase contrast image reveals only a slight distinction between the gray and white matter, this is due to the relatively weak scattering of brain tissue. In comparison, the differences between the two are quite visible with the present method. This can be attributed to the biological differences in the composition of the two tissue types, which give rise to a small but measurable refractive index dispersion change.

[0029] Phase dispersion methods can also be used for 3D imaging, by employing a backscattering geometry. This provides tomographic phase dispersion images on *in-vivo* sites. This technique is very sensitive to small biological differences that manifest themselves as changes in the index of refraction. In addition, simultaneous measurement of the amplitude and phase of the heterodyne signals yields the real and imaginary parts of the refractive index, providing a more complete set of data about the scanned sample.

[0030] As seen in Figure 6B, the upper left panel shows the structure to be imaged, the lower two panels show OCT images at 800 nm and 400 nm which fail to discriminate between gelatin and water. The upper right panel shows a differential phase image of the structure which in the lower band of the image clearly features the gelatin/water boundary after the light reflects off the mirror.

[0031] Thus, by spectrally scanning the fundamental/second harmonic wavelength, precise scatterer size distributions in tissue can be measured. The size characterization can far exceed the actual voxel resolution, as phase-based measurements are very sensitive to the spectral variation of the refractive index with scatterer size. This method complements related intensity-based techniques by rendering three dimensional images of the size distribution and chromatin content of cell nuclei which are important indicators of pre-cancerous or cancerous changes in biological tissues.

[0032] In a first embodiment both wavelengths need to be from low coherence sources. For example, a femtosecond Ti:sapphire laser source and its second harmonic generation. Another example, is two superluminescent diodes of appropriate wavelengths. In this manifestation, both wavelengths penetrate to the same scanned depth and are scattered/reflected back. Their relative phase is then measured after they interfere with their respective reference arm components to form heterodyne signals.

[0033] In another preferred embodiment illustrated in Figure 7, is a 3D phase imaging system 50 in which only one wavelength needs to be from a low coherence source 52. The second wavelength may be form a coherent continuous wave 54 (CW) (or any other coherent source). The additional requirement is that the coherence length of the source is greater than the total length of the depth scan.

[0034] In this situation, the reflected component 64 of this light source, from the target's dominant reflecting/scattering surface 60, interferes with its reference arm component and generates a continuous heterodyne signal during depth wise scan of the target tissue 68. Its phase may then be used in a similar manner described above to eliminate jitter noises from the low coherence component of the pair of light sources. The low coherence component penetrates to the scanned depth and are reflected/scattered back. It forms a heterodyne signal with its reference arm component. In the embodiment in which two low coherence sources are used as described above in this imaging system, both wavelengths penetrate and are reflected and/or scattered by the tissue.

[0035] Illustrated in connection with Figure 8 is a fiber optic system 200 for light delivery and/or collection in conjunction with the light scattering spectroscopic systems and methods of the invention described previously. A light source provides a beam 202 that includes at least two wavelengths λ_1, λ_2 which are coupled to the proximal end of optical fiber 204. A beam splitter 206 incorporated into the fiber optic system delivers light components through fibers 208 and 210, and through lenses 216 and 214, respectively. A first light component is reflected by moving mirror 220 traveling in direction 220, and returns through fibers 210 and 212. A second light component is directed onto tissue 218, and light scattered by the tissue is returned through fibers 208 and 212. Dichroic mirror 230 separates the two wavelength λ_1 and λ_2 which are detected by detectors 240 and 242, respectively.

The heterodyne detection systems 250 and 252 are used to process the detected systems as described previously in connection with Figure 1. The systems described herein can be used in conjunction with standard endoscopics to provide diagnostic information retrieved from lumens or tissue within the human body *in vivo.*

Claims

1. A device for optically measuring a medium comprising:-

a light source (14) arranged to provide a first wavelength and a second wavelength of light such that the second wavelength harmonically related to the first wavelength;
an optical system (23, 206) arranged to couple light of the first wavelength and the second wavelength along both a first optical path and a second optical path, the first optical path extending onto a medium (18) be measured and the second path undergoing a change in path length; **characterized in that**
a detector (D1, D2) arranged to detect light from the medium and light from the second optical path and to measure a phase difference between the first wavelength and the second wavelength of light interacting with the medium.

2. The device of Claim 1 arranged for optically measuring a medium (18) comprising biological tissue.

3. The device of Claim 1 further comprising a data processor (26) arranged to determine a size of a particle within the medium (18).

4. The device of Claim 1 further comprising a data processor (26) arranged to form an image of the medium (18) with the detected scattered light

5. The device of Claim 1 further comprising a data processor (26) arranged to determine a change in phase velocity of light interacting with the medium (18).

6. The device of Claim 1 wherein the light source (14) is arranged to emit light in the visible and near-infrared regions.

7. The device of Claim 1 further comprising a first low coherence (52) light source and a second low coherence light source (54).

8. The device of Claim 1 further comprising a low coherence light source (52) and a coherent light source (54).

9. The device of Claim 1 wherein the second wavelength is within 5% of an integer multiple of the first wavelength,

10. The device of Claim 1 further comprising a fiber optic device (200) arranged to couple light from the light source onto the medium (218).

11. The device of Claim 1 further comprising a fiber optic device (200) arranged to that couple light from the medium (218) to the detector (240, 242).

12. The device of Claim 1 wherein the detector comprises a first photodetector (240) and a second photodetector (242).

13. The device of Claim 1 further comprising a compensatory (15).

14. The device of Claim 1 further comprising a first scanning mirror (M1) arranged to reflect light on the second optical path and a second mirror reflecting light on the first optical path (M2).

15. The device of Claim 1 further comprising a beam splitter (BS) and a plurality of lenses (O1, O2).

16. The device of Claim 1 further comprising an analog to digital converter (ADC) connected to the detector (D1, D2).

17. The device of Claim 1 further comprising a heterodyne detection system.

18. The device of Claim 1 further comprising a fiber optic probe and an endoscope.

19. The device of Claim 1 wherein the light source (14) comprises a continuous wave laser.

20. A method for optically measuring a medium (18) comprising:

providing a first wavelength and a second wavelength of light such that the second wavelength is harmonically related to the first wavelength;
directing light of the first wavelength and the second wavelength along both a first optical path and a second optical path, the first optical path extending onto a medium (18) to be measured and the second path undergoing a change in path length **characterized in**
detecting light from the medium and light from the second optical path to measure a phase difference between the first wavelength and the second wavelength of light interacting with the medium.

21. The method of Claim 20 wherein the medium (18) comprises a light scattering medium.

22. The method of Claim 20 further comprising determining a size of a particle within the medium (18).

23. The method of Claim 20 further comprising forming an image of the medium (18) with the detected scattered light.

24. The method of Claim 20 further comprising measuring a change in phase velocity of light interacting with the medium (18).

25. The method of Claim 20 further comprising providing light source (14) that emits the first wavelength and a second wavelength that are harmonically related.

26. The method of Claim 20 further comprising providing a first low coherence light source (52) and a second low coherence light source (54).

27. The method of Claim 20 further comprising providing a low coherence light source (52) and a coherent light source (54).

28. The method of Claim 20 wherein the second wavelength is within 5% of an integer multiple of the first wavelength.

Patentansprüche

1. Apparat zur optischen Messung eines Mediums umfassend:

   eine Lichtquelle (14), so angeordnet, dass sie Licht mit einer ersten Wellenlänge und einer zweiten Wellenlänge liefert, so dass die zweite Wellenlänge harmonisch zu der ersten Wellenlänge ist;
   ein optisches System (16, 200), so angeordnet, dass es Licht mit der ersten Wellenlänge und der zweiten Wellenlänge entlang sowohl eines ersten optischen Wegs als auch eines zweiten optischen Wegs koppelt, wobei sich der erste optische Weg auf ein zu messendes Medium (18) erstreckt, und der zweite Weg eine Änderung in der Wegstrecke erfährt; **dadurch gekennzeichnet, dass**
   ein Detektor (D1, D2) angeordnet ist, um Licht vom Medium und Licht vom zweiten optischen Pfad zu detektieren, und um eine Phasendifferenz zwischen der ersten Wellenlänge und der zweiten Wellenlänge von Licht, das mit dem Medium wechselwirkt, zu messen.

2. Apparat von Anspruch 1, angeordnet um ein Medium (18), das biologisches Gewebe umfasst, optisch zu vermessen.

3. Apparat von Anspruch 1, ferner umfassend einen Datenprozessor (26), der angeordnet ist, um eine Größe eines Teilchens in dem Mediums (18) zu bestimmen.

4. Apparat von Anspruch 1, ferner umfassend einen Datenprozessor (26), der angeordnet ist, um ein Bild des Mediums (18) mit dem detektierten Streulicht darzustellen.

5. Apparat von Anspruch 1, ferner umfassend einen Datenprozessor (26), der angeordnet ist, um eine Änderung der Phasengeschwindigkeit von Licht, das mit dem Medium (18) wechselwirkt, zu ermitteln.

6. Apparat von Anspruch 1, wobei die Lichtquelle (14) angeordnet ist, um Licht in den sichtbaren und nahen Infrarot-Bereichen zu emittieren.

7. Apparat von Anspruch 1, ferner umfassend eine erste niedrigkohärente (52) Lichtquelle und eine zweite niedrigkohärente Lichtquelle (54).

8. Apparat von Anspruch 1, ferner umfassend eine niedrigkohärente Lichtquelle (52) und eine kohärente Lichtquelle (54).

9. Apparat von Anspruch 1, wobei die zweite Wellenlänge innerhalb von 5% eines ganzzahligen Vielfachen der ersten Wellenlänge ist.

10. Apparat von Anspruch 1, ferner umfassend eine Faseroptik-Anordnung (200) die angeordnet ist, um Licht von der Lichtquelle zum Medium (218) zu koppeln.

11. Apparat von Anspruch 1, ferner umfassend eine Faseroptik-Anordnung (200), die angeordnet ist, um Licht vom Medium (218) zum Detektor (240, 242) zu koppeln.

12. Apparat von Anspruch 1, wobei der Detektor einen ersten Photodetektor (240) und einen zweiten Photodetektor (242) umfasst.

13. Apparat von Anspruch 1, ferner umfassend einen Kompensator (15).

14. Apparat von Anspruch 1, ferner umfassend einen ersten Scanning-Spiegel (M1), der angeordnet ist, um Licht auf den zweiten optischen Weg zu reflektieren, und einen zweiten Spiegel, der Licht auf den ersten optischen Pfad reflektiert (M2).

15. , Apparat von Anspruch 1, ferner umfassend einen Strahlteiler (BS) und eine Vielzahl von Linsen (O1, O2).

16. Apparat von Anspruch 1, ferner umfassend einen Analog-Digital-Wandler (ADC), der mit dem Detektor (D1, D2) verbunden ist.

17. Apparat von Anspruch 1, ferner umfassend ein Überlagerungs-Detektionssystem.

18. Apparat von Anspruch 1, ferner umfassend eine Faseroptik-Sonde und ein Endoskop.

19. Apparat von Anspruch 1, wobei die Lichtquelle (14) einen kontinuierlichen Laser umfasst.

20. Verfahren zur optischen Messung eines Mediums (18), bei dem man:

Licht mit einer ersten Wellenlänge und einer zweiten Wellenlänge vorsieht, so dass die zweite Wellenlänge einen harmonischen Bezug zur ersten Wellenlänge aufweist;
Licht mit der ersten Wellenlänge und der zweiten Wellenlänge entlang sowohl eines ersten optischen Wegs als auch eines zweiten optischen Wegs lenkt, sich der erste optische Weg bis zum zu messenden Medium (18) erstreckt, und der zweite Weg eine Änderung in der Wegstrecke etfährt; **dadurch gekennzeichnet, dass** man
Licht vom Medium und Licht vom zweiten optischen Weg detektiert, um eine Phasendifferenz zwischen der ersten Wellenlänge und der zweiten Wellenlänge von Licht, das mit dem Medium wechselwirkt, zu messen.

21. Verfahren von Anspruch 20, wobei das Medium (18) ein lichtstreuendes Medium umfasst.

22. Verfahren von Anspruch 20, ferner umfassend die Bestimmung einer Größe eines Teilchens in dem Medium (18).

23. Verfahren von Anspruch 20, ferner umfassend die Darstellung eines Bildes des Mediums (18) mit dem detektierten Streulicht.

24. Verfahren von Anspruch 20, ferner umfassend das Messen einer Änderung der Phasengeschwindigkeit von Licht, das mit dem Medium (18) wechselwirkt.

25. Verfahren von Anspruch 20, ferner umfassend das Bereitstellen einer Lichtquelle (14), die die erste Wellenlänge und eine zweite Wellenlänge, die harmonischen Bezug aufweisen, emittiert.

26. Verfahren von Anspruch 20, ferner umfassend das Bereitstellen einer ersten niedrigkohärenten Lichtquelle (52) und einer zweiten niedrigkohärenten Lichtquelle (54).

27. Verfahren von Anspruch 20, ferner umfassend das Bereitstellen einer niedrigkohärenten Lichtquelle (52) und einer kohärenten Lichtquelle (54).

28. Verfahren von Anspruch 20, wobei die zweite Wellenlänge innerhalb von 5% eines ganzzahligen Vielfachen der ersten Wellenlänge ist.

Revendications

1. Dispositif de mesure optique d'un milieu comprenant :

une source lumineuse (14) agencée pour produire une première longueur d'onde et une deuxième longueur d'onde de lumière, de telle sorte que la deuxième longueur d'onde est en relation harmonique avec la première longueur d'onde ;
un système optique (16, 206) agencé pour coupler la lumière de la première longueur d'onde et de la deuxième longueur d'onde, le long d'un premier chemin optique et d'un deuxième chemin optique, le premier chemin optique s'étendant sur un milieu (18) à mesurer et le deuxième chemin subissant un changement de longueur de chemin ; **caractérisé en ce que**
un détecteur (D1, D2) agencé pour détecter la lumière d'un milieu et la lumière d'un deuxième chemin optique, et pour mesurer une différence de phase entre la première longueur d'onde et la deuxième longueur d'onde de lumière interagissant avec le milieu.

2. Dispositif selon la revendication 1, agencé pour mesurer de façon optique un milieu (18) comprenant un tissu biologique.

3. Dispositif selon la revendication 1, comprenant en outre un processeur de données (26) agencé pour déterminer la dimension d'une particule à l'intérieur du milieu (18).

4. Dispositif selon la revendication 1, comprenant en outre un processeur de données (26) agencé pour former une image du milieu (18) à l'aide de la lumière diffusée détectée.

5. Dispositif selon la revendication 1, comprenant en outre un processeur de données (26) agencé pour changer la vitesse de phase de la lumière interagissant avec le milieu (18).

6. Dispositif selon la revendication 1. dans lequel la source lumineuse (14) est agencée pour émettre une lumière dans les régions visible et proche infrarouge.

7. Dispositif selon la revendication 1. comprenant en outre une première source lumineuse peu cohérente (52) et une deuxième source lumineuse peu cohérente (54).

8. Dispositif selon la revendication 1, comprenant en outre une source lumineuse peu cohérente (52) et une source lumineuse cohérente (54).

9. Dispositif selon la revendication 1, dans lequel la deuxième longueur d'onde est un nombre entier multiple dans les limites de 5% de la première longueur d'onde.

10. Dispositif selon la revendication 1, comprenant en outre un dispositif à fibre optique (200) agencé pour coupler la lumière de la source lumineuse au milieu (218).

11. Dispositif selon la revendication 1, comprenant en outre un dispositif à fibre optique (200) agencé pour coupler la lumière du milieu (218) au détecteur (240, 242).

12. Dispositif selon la revendication 1, dans lequel le détecteur comprend un premier photodétecteur (240) et un deuxième photodétecteur (242).

13. Dispositif selon la revendication 1, comprenant en outre un compensateur (15).

14. Dispositif selon la revendication 1, comprenant en outre un premier miroir de balayage (ml) agencé pour refléter la lumière sur le deuxième chemin optique, et un deuxième miroir (m2) reflétant la lumière sur le premier chemin optique .

15. Dispositif selon la revendication, comprenant en outre un séparateur de faisceaux (BS) et une pluralité de lentilles (01, 02).

16. Dispositif selon la revendication 1, comprenant en outre un convertisseur analogique-numérique (ADC) relié au détecteur (D1, D2).

17. Dispositif selon la revendication 1, comprenant en outre un système de détection hétérodyne.

18. Dispositif selon la revendication 1, comprenant en outre une sonde à fibre optique et un endoscope.

19. Dispositif selon la revendication 1, dans lequel la source lumineuse (14) comprend un laser à onde continue.

20. Procédé de mesure optique d'un milieu (18) comprenant :

la fourniture d'une première longueur d'onde et d'une deuxième longueur d'onde, de telle sorte que la deuxième longueur d'onde est en relation harmonique avec la première longueur d'onde ;
l'orientation de la lumière de la première longueur d'onde et de la deuxième longueur d'onde le long d'un premier chemin optique et d'un deuxième chemin optique, le premier chemin optique s'étendant sur un milieu (18) à mesurer et le deuxième chemin subissant un changement de longueur de chemin, **caractérisé en**
la détection de la lumière du milieu et de la lumière du deuxième chemin optique pour mesurer une différence de phase entre la première longueur d'onde et la deuxième longueur d'onde de lumière interagissant avec le milieu.

21. Procédé selon la revendication 20. dans lequel le milieu (18) comprend un milieu de diffusion de la lumière.

22. Procédé selon la revendication 20. comprenant en outre la détermination de la dimension d'une particule à l'intérieur du milieu (18).

23. Procédé selon la revendication 20. comprenant en outre la formation d'une image du milieu (18) à l'aide de la lumière diffusée détectée.

24. Procédé selon la revendication 20, comprenant en outre la mesure d'un changement de vitesse de phase de la lumière interagissant avec le milieu (18).

25. Procédé selon la revendication 20. comprenant en outre la fourniture de la source lumineuse (14) qui émet la première longueur d'onde et une deuxième longueur d'onde qui sont en relation harmonique.

26. Procédé selon la revendication 20, comprenant en outre la fourniture d'une première source lumineuse peu cohérente (52) et d'une deuxième source lumineuse peu cohérente (54).

27. Procédé selon la revendication 20, comprenant en outre la fourniture d'une source lumineuse peu cohérente (52) et d'une source lumineuse cohérente (54).

28. Procédé selon la revendication 20, dans lequel la deuxième longueur d'onde est égale à un nombre entier multiple dans les limites de 5% de la première longueur d'onde.

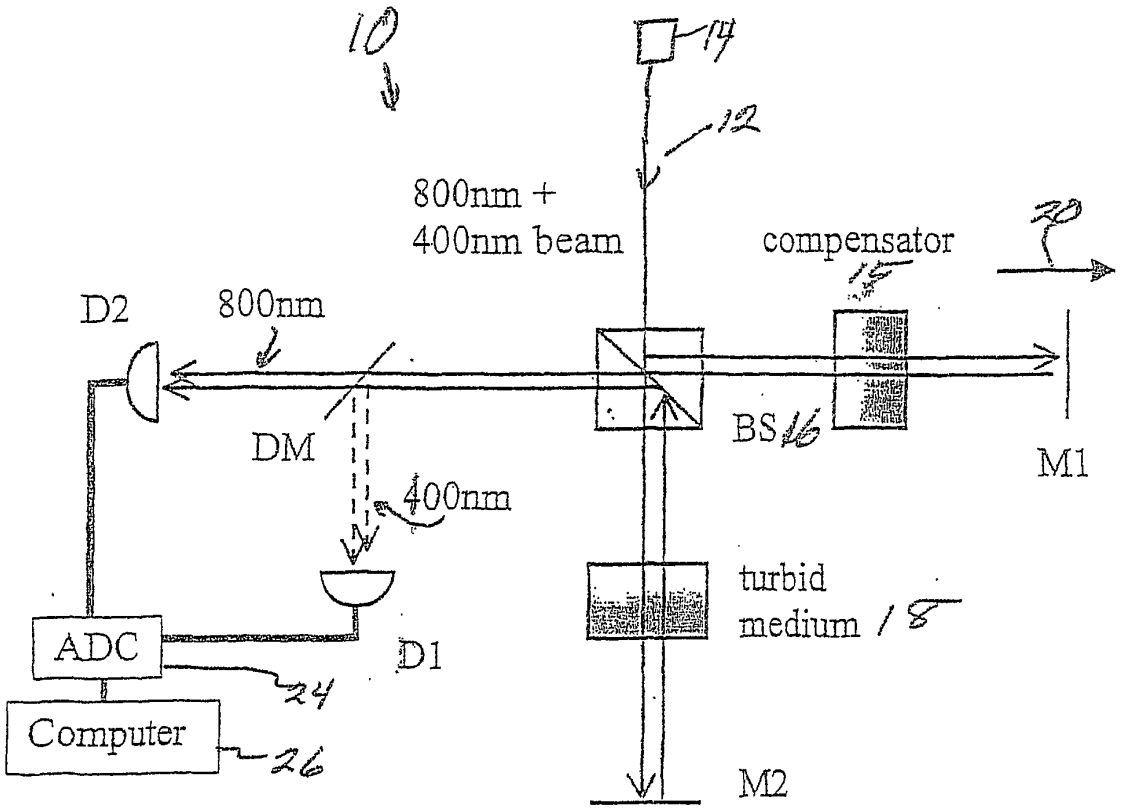
10
14
12
800nm +
400nm beam
compensator
30
D2
800nm
15
DM
BS 16
M1
400nm
turbid
medium 18
ADC
D1
24
Computer
26
M2

Figure 1

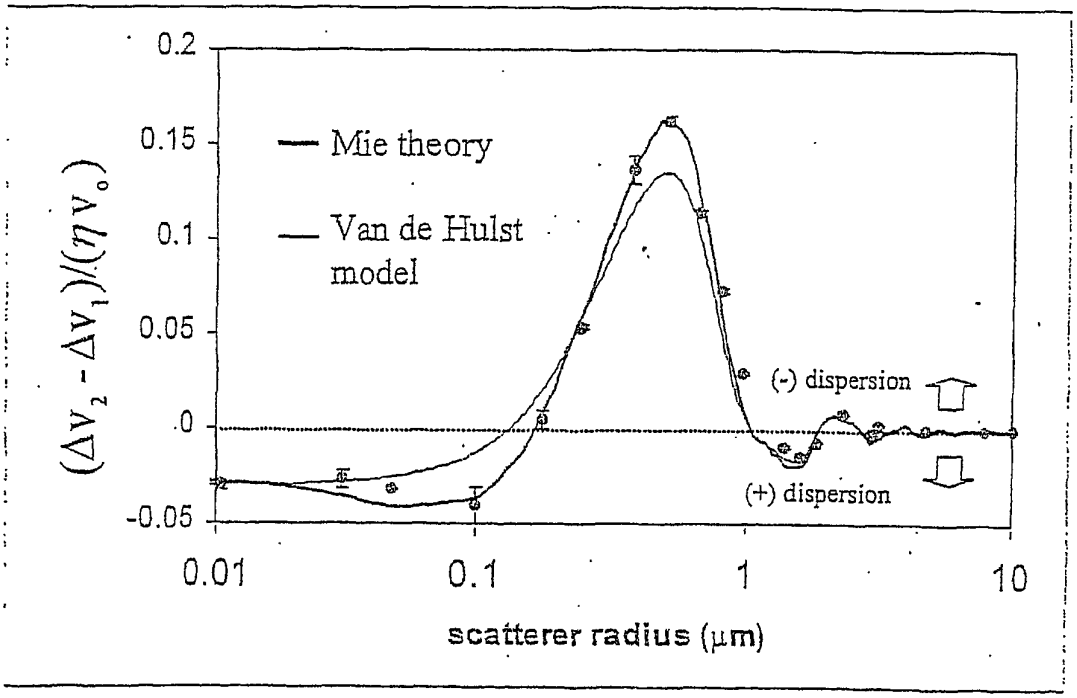
0.2
0.15
0.1
0.05
0
-0.05
0.01
0.1
1
10
Mie theory
Van de Hulst model
(-) dispersion
(+) dispersion
$(\Delta\nu_2 - \Delta\nu_1)/(\eta\nu_o)$
scatterer radius (μm)

Figure 2

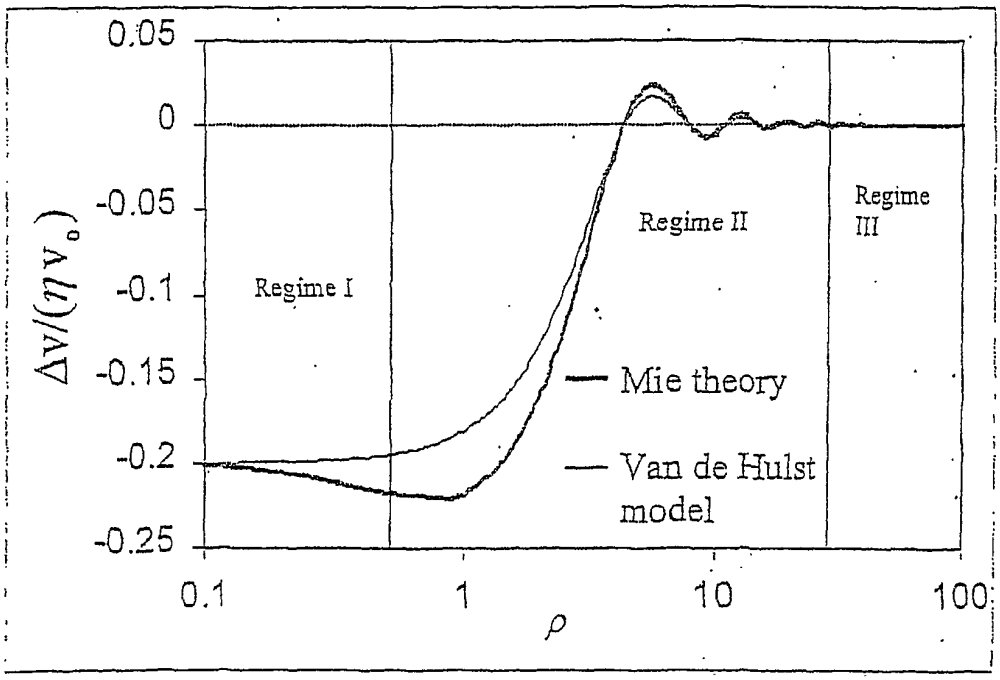
0.05
0
-0.05
-0.1
-0.15
-0.2
-0.25
$\Delta v/(\eta v_o)$
Regime I
Regime II
Regime III
Mie theory
Van de Hulst model
0.1
1
10
100
ρ

Figure 3

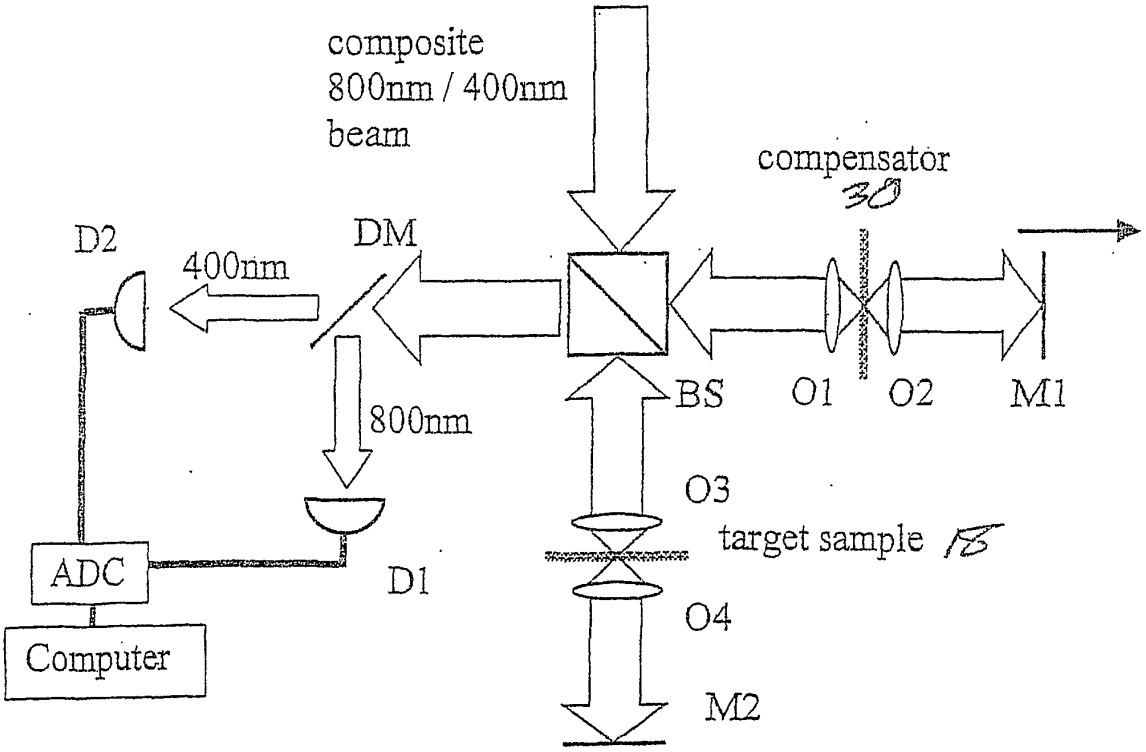
composite
800nm / 400nm
beam
compensator
30
D2
400nm
DM
BS
O1
O2
M1
800nm
O3
target sample
15
ADC
D1
O4
Computer
M2

Figure 4

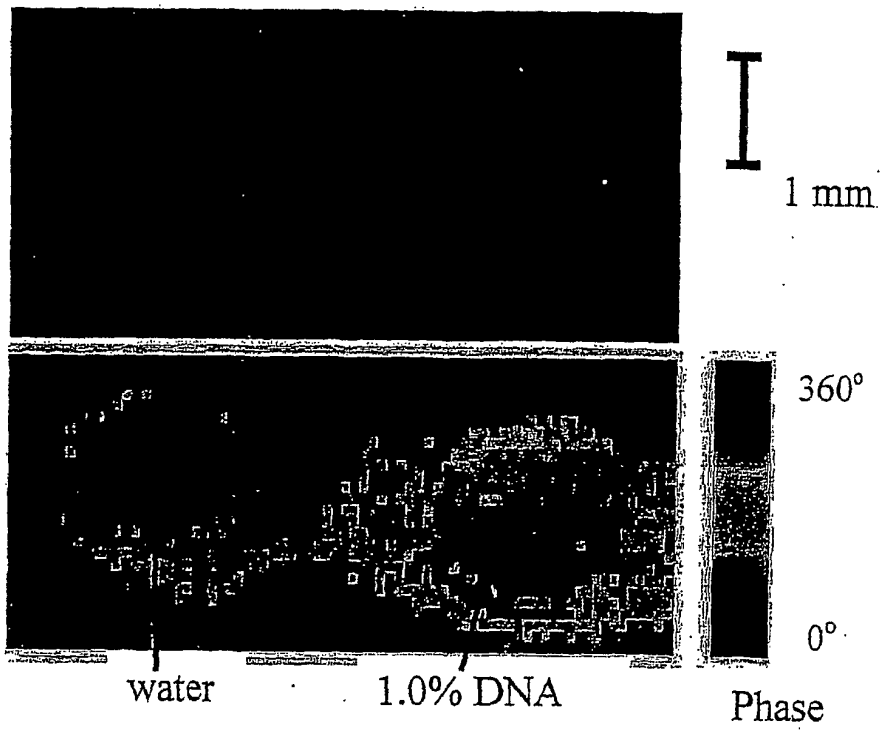

Figure 5

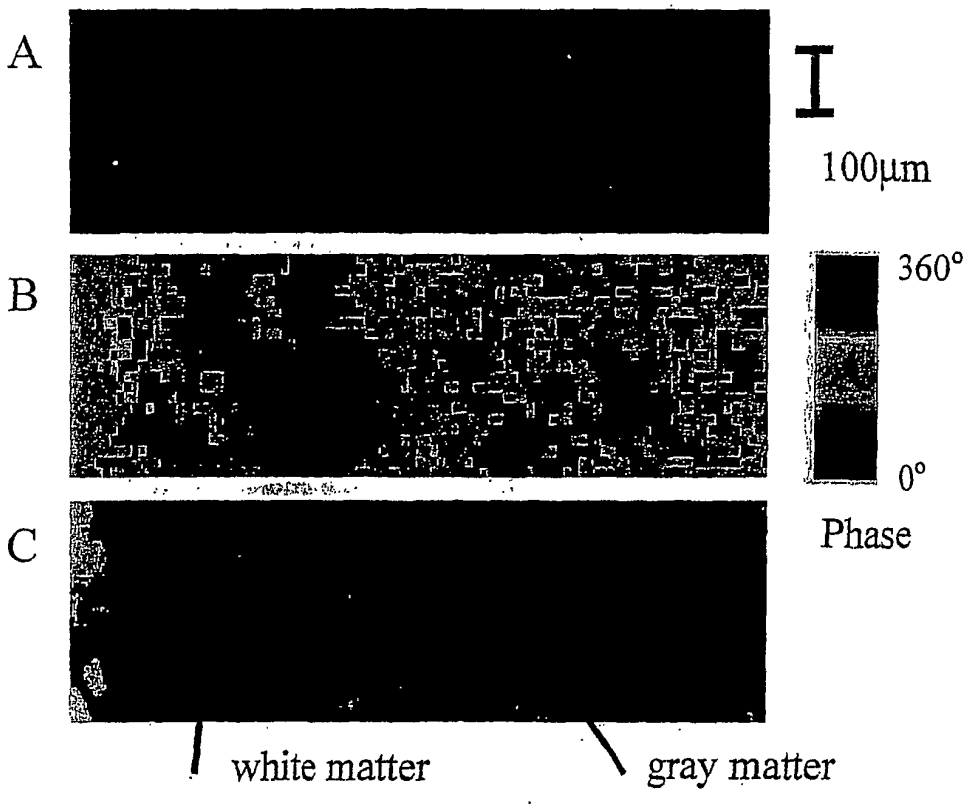

Figure 6A

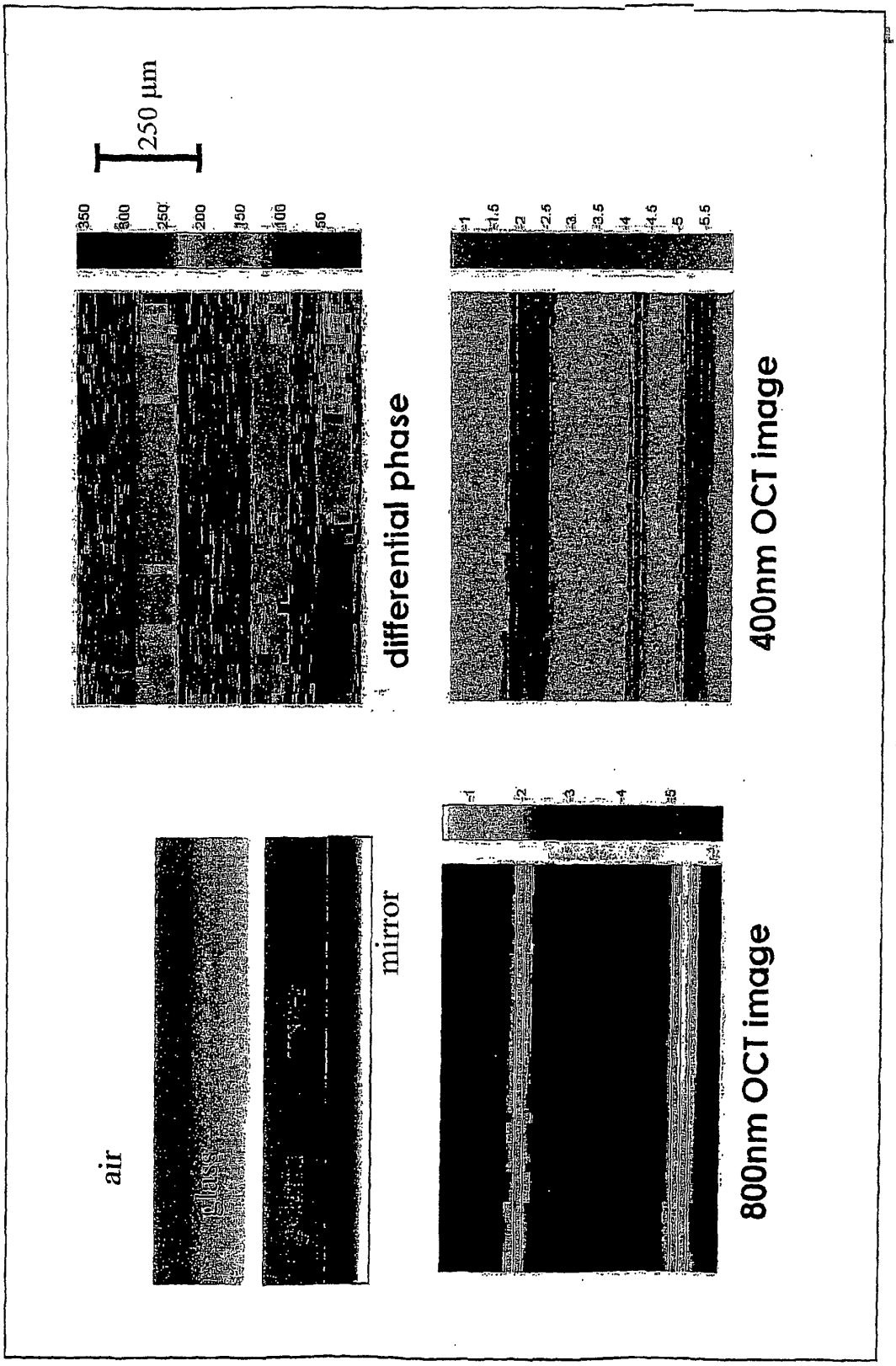
250 µm
350
300
250
200
150
100
50
differential phase
-1
-1.5
-2
-2.5
-3
-3.5
-4
-4.5
-5
-5.5
400nm OCT image
air
glass
mirror
800nm OCT image

Figure 6B

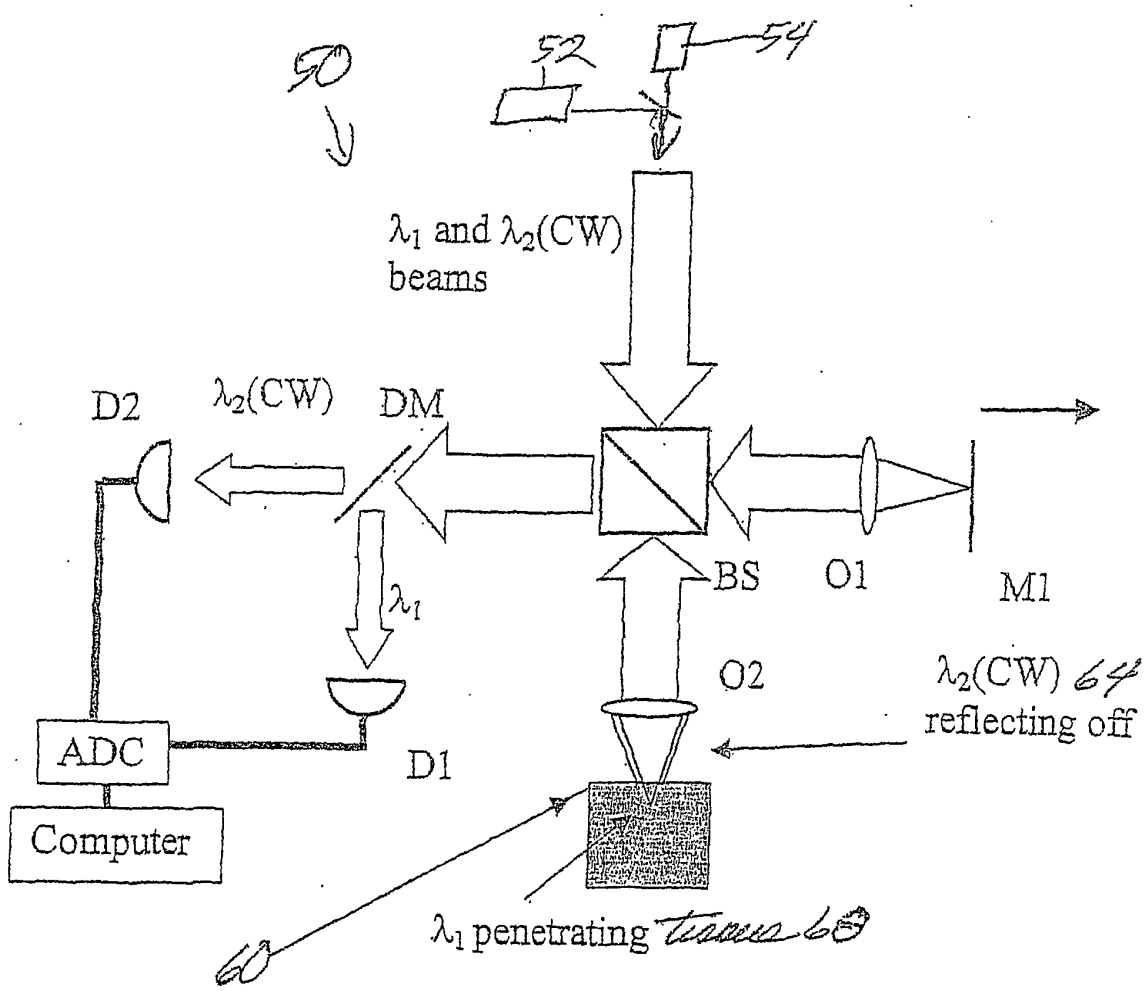
50
52
54
λ1 and λ2(CW) beams
D2
λ2(CW)
DM
BS
O1
M1
λ1
O2
λ2(CW) 64 reflecting off
ADC
D1
Computer
λ1 penetrating tissue 68
60

Figure 7

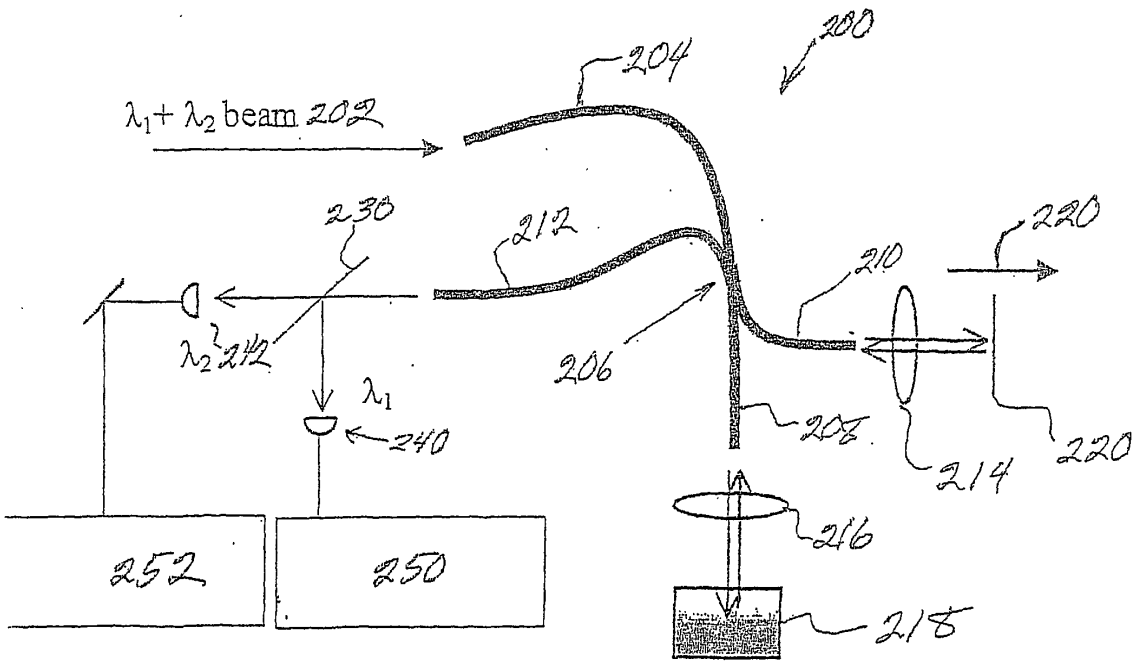
200
204
λ1+ λ2 beam 202
230
212
210
220
λ2
λ1
240
206
207
214
220
216
252
250
218

Figure 8

专利名称(译)	相位色散断层扫描		
公开(公告)号	EP1305601B1	公开(公告)日	2005-12-21
申请号	EP2001942160	申请日	2001-06-08
[标]申请(专利权)人(译)	麻省理工学院		
申请(专利权)人(译)	麻省理工学院		
当前申请(专利权)人(译)	麻省理工学院		
[标]发明人	YANG CHANGHUEI WAX ADAM FELD MICHAEL S		
发明人	YANG, CHANGHUEI WAX, ADAM FELD, MICHAEL, S.		
IPC分类号	G01N21/17 A61B5/00 G01N15/02 G01N21/47 G02B21/14		
CPC分类号	A61B5/0073 A61B5/0066 G01N15/0205 G01N21/4795		
优先权	09/591297 2000-06-09 US		
其他公开文献	EP1305601A2		
外部链接	Espacenet		

摘要(译)

通过混浊介质未偏转传播的辐射由于其波动性质而经历相速度的微小变化。可以使用差分相位光学干涉仪测量该变化。弹道传播可分为三种方式：对于与波长相比较小的散射体，混浊介质充当大块介质;对于大型散射体，相速度与浊度无关;在中间状态下，相速度强烈依赖于散射体半径。特别地，对于具有中等尺寸的散射体，通过添加较高折射率的正色散散射体观察到相速度增加和负色散。这些测量是使用基波和谐波之间的相位差进行的，可用于提供组织或生物流体的诊断信息和图像。